Chapter 1

1.1 Introduction

Transparent conducting oxides (TCO) are a unique subset of semiconductors that exhibit both transparency in the visible range and conductivity. Due to the unique combination of properties, TCOs find applications in many optoelectronic devices such as solar cells, display devices, light-emitting devices, etc.

Transparent conducting oxide (TCO) was first synthesized in 1907 by Badeker when he was successful in depositing cadmium oxide (CdO) film, having resistivity ~10^{-3} Ω-cm, by thermal evaporation [1]. Since then, several oxide TCO systems have been developed mainly based on cadmium oxide (CdO), indium oxide (In_2O_3), tin oxide (SnO_2), zinc oxide (ZnO), and gallium oxide (Ga_2O_3) [2]. Among all the TCOs, indium tin oxide (ITO) is commercially most successful, mainly due to its higher transparency (~>91%) and conductivity (~>10^3 S/cm) [3]. However, indium sources are scarce, making them costly [4]. At the same time, compounds of indium are toxic [5], which is not sustainable for the ever-increasing demand for TCO for the growing optoelectronic industry. Therefore, TCO based on non-toxic earth-abundant elements is being sought. Being abundant and biocompatible, ZnO is among the most sought alternative. ZnO exhibits all the essential properties for a good TCO including a wide bandgap of ~3.34 eV and a high exciton binding energy of 60 meV. To increase the conductivity ZnO has been doped with several group IIIA and IVA elements including Al, B, In, Ga, Sn, and Si [6]. ZnO films were

deposited first time in 1966 by R. A. Mickelsen using reactive magnetron sputtering [7], while Nobbs and Gillespie deposited ZnO by spray pyrolysis [8] in 1970. Aranovich et al., in 1980, was the first to utilize ZnO as a conductive layer over CdTe film using spray pyrolysis to form a heterojunction solar cell [9]. Since then, doped and intrinsic ZnO thin films have been established as a regular component of many optoelectronic devices.

Crystallographic orientation, microstructure, and defects, which depend on processing history, play an important role in deciding the functional properties of ZnO-based TCOs. For instance, it has been observed that films processed by Vapor-based techniques (such as sputtering, pulsed laser deposition, chemical vapor deposition, etc.) can result in compact, (002) oriented large-grained films, exhibit greater conductivity, and transparency [10–13]. Resistivity in the range $\sim 10^{-4}$ to 10^{-5} Ω-cm and transparency ≥88% have been reported for Al-doped ZnO processed through pulse laser deposition (PLD) and sputtering [14–19]. However, vapor-based processing routes are costly and are not easily implementable for large-scale production. Therefore, several researchers have tried to develop solution-based processing techniques for ZnO-based TCOs with limited success in achieving performance at par with the vapor-based processes [20–23]. Solution based processing methods include spin coating[24–26], dip coating [27,28], chemical bath deposition [29,30], spray pyrolysis [31–33], and chemical vapor deposition (CVD)[17] .

The main objective of this thesis work is to develop high throughput, solution-based processing protocols for achieving conductivity and transparency of Al-doped ZnO films close to that reported through the vapor-based processing routes.

1.2 Transparent conductive oxide (TCO)

Transparent conductive oxide has a unique combination of electrical conductivity and transparency in the visible range. Visible light has wavelengths in the range of about 400-750 nm or energy in the range of 1.7-3.1 eV. An object can be optically transparent if no reflection or absorption occurs in the visible spectral range. In semiconductors with a bandgap larger than 3.1 eV, inter-band transitions do not occur in the visible light range (wavelength 400-700 nm); visible light can pass through them without being absorbed [2]. However, such materials in their nascent form have very high resistivity of the order $>\sim 10^2$ Ω-cm [20]. These materials can be made conductive by doping or introducing defects levels with extra electrons close to the conduction band minima. Such conductive and transparent materials can serve as front contacts for thin-film hetero-structured optoelectronic devices [34]. For the better performance of TCOs having resistivity lower than $\sim 10^{-2}$ Ω-cm along with the ~>85% transparency in the visible range is needed [35,36].

1.3 Fundamentals of TCOs

TCOs are electrically conductive, at the same time, transparent. Conductivity and transparency are mutually exclusive properties of thin film solids. Understanding the behavior of electrons in solids is important to explain this unusual behavior of TCOs. Band theory is a convenient way to explain the electrical properties of TCOs [37].

1.3.1 Band Theory

The energy of electrons in an atom is quantized in orbitals. When more than one atom or molecule is brought together, their electronic orbitals start to overlap. However, two electrons cannot have the same energy; therefore, the energy levels split with tiny differences to satisfy Pauli's exclusion principle, as shown schematically in **Figure 1.1**. When a large number of atoms are assembled to form a solid, the atomic orbitals split into a large number of states, with very little difference in energy, resulting in the formation of what is known as energy bands, as shown in **Figure 1.2**. The highest filled energy band is known as valance band maxima (VBM), while the lowest unoccupied energy band is known as conduction band minima (CBM). The energy gap between the highest filled valance band and the lowest unoccupied conduction band is known as a bandgap. Depending upon the bandgap, a solid is classified as an insulator, a semiconductor, or a metal. Materials with bandgap > ~ 4 eV are classified as an insulator. Materials with a bandgap < 4 eV are classified as semiconductors, while materials with overlapping conduction and valance band or partially filled conduction bands are known as metals.

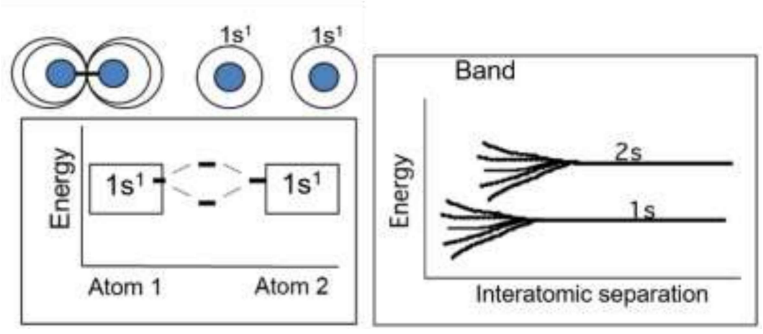

Figure 1.1 Schematic of inter-band splitting

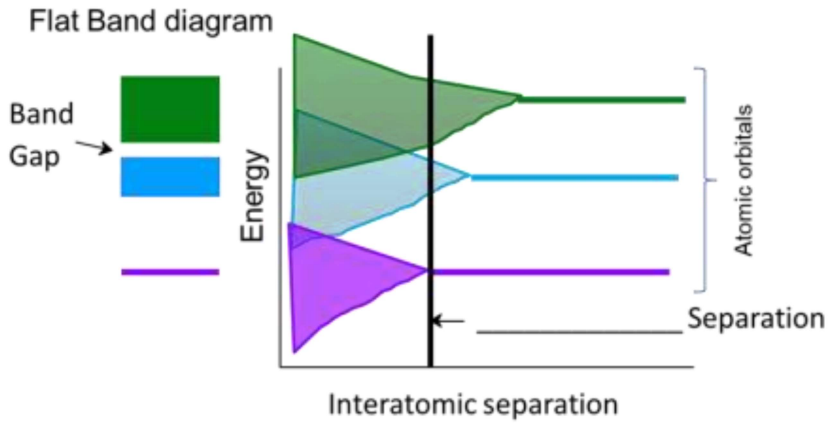

Figure 1.2 Band splitting in semiconductor material with interatomic separation

1.3.2 Conductivity

In the case of metals, the conduction band and the valance band are overlapped; therefore, the electrons can easily jump into the conduction band and conduct electricity even under a small applied electrical potential. However, semiconductors require additional stimulation to excite electrons from the valance band to the conduction band. Therefore, the conductivity of semiconductors is usually much lower than metals. On supplying energy through external sources, such as heating or under the effect of irradiation having energy comparable to or higher than the bandgap, more electrons can be stimulated into the conduction band, thereby increasing the conductivity. On the other hand, since the bandgap of an insulator is wider than a semiconductor ($\geq$4 eV), generally, under normal conditions and below a threshold voltage, no conduction is observed.

1.3.3 Fermi level

Fermi level (E_f) is the highest energy level occupied by electrons at absolute zero kelvin. In the case of metal, the Fermi level is within the conduction band (due to band overlap); therefore, the electrons are free to move even under a very small applied potential. On the other hand, in the case of semiconductor Fermi level fall close to the middle of the bandgap. At higher temperature, electrons are excited (when the energy supplied to electrons are comparable to the bandgap) to mobilize more electrons. Doping is another way of introducing electrons close to the conduction band, which can easily be ionized to give metal-like conductivity.

1.3.4 Drude model of conductivity

A model was proposed by Paul Drude in 1900, originally to explain the transport properties of electrons in metals, commonly known as the Drude Model. It can also be effectively applied in the case of doped semiconductors [38]. Drude model assumes that the electrons move in a straight line, and electrons achieve thermal equilibrium with the lattice through collision, as shown in **Figure 1.3**.

TCO is used in optoelectronic devices, which deal with the direct current and follow Ohm's law. According to Ohms' law, the current (I) flowing through a conductor is proportional to the applied voltage (V).

$$V = IR \qquad 1.1$$

where R is the resistance of the conductor. Dividing both sides by the cross-sectional area of the conductor, the Ohm law can be expressed in terms of electric field (E) and current density (J):

$$E = \rho J \qquad 1.2$$

where ρ is the resistivity of the conductor.

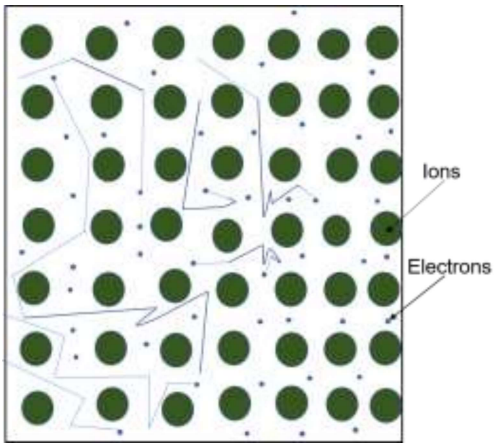

Figure 1.3 Drude Model

If the number of electrons with velocity *v* crossing area A in a time interval dt is *nvAdt*, the current density can be given by:

$$J = -nev \tag{1.2}$$

The velocity of the electron under the applied electric field E is given by:

$$v = -\frac{eE\tau}{m^*} \tag{1.3}$$

$$J = -nev = \frac{ne^2\tau}{m^*}E \tag{1.4}$$

where τ is the time since the last collision; comparing equations (1.3) and (1.4)

$$\sigma = \frac{ne^2\tau}{m^*} = n\mu e \tag{1.5}$$

where $\frac{e\tau}{m^*}$ is termed mobility (μ).

Therefore, the conductivity of a semiconductor can be increased by increasing the number of charge carriers or mobility or by reducing the rest mass of the electron (m^*).

1.3.5 Optical properties

Semiconductor materials can either absorb, reflect, or allow the incident radiation to pass through them, depending upon the bandgap of the semiconductor and the energy (or frequency). When the energy of the incident radiation is less than the bandgap, the electron cannot be excited to the conduction band; therefore, no absorption takes place. For such wavelengths, the semiconductor is considered transparent. On the other hand, when the energy of the incident radiation is sufficient ($E_{photon} > E_g$) to excite the valance band electrons across the bandgap into the conduction band, the radiation is absorbed by the semiconductors giving rise to a hole in the valence band, and a free electron into the conduction band. This excited electron can again come back to the ground state by giving up energy through radiative or non-radiative processes. The emission of radiation during de-excitation is called photoluminescence. Therefore, the semiconductors are transparent to the wavelengths (λ) greater than that corresponding to the bandgap ($\lambda_g \approx 1240/E_g$).

Semiconductors behave like insulators at high frequencies (i.e lower wavelengths), while at low frequencies (i.e. high wavelengths), it starts behaving like metals. The frequencies below a threshold are reflected. The threshold frequency at which this transition happens is known as plasma frequency (ω_p). While the radiation having frequencies higher than plasma frequency is transmitted. On the other hand, photons having energies (or frequency) higher than the bandgap are absorbed. The

transmittance, absorbance, and reflectance for a typical TCO film are depicted in **Figure 1.4**. The plasma frequency is given by equation 1.6

$$\omega_p = \sqrt{\frac{ne^2}{\epsilon_o\, m_e^*}} \qquad 1.6$$

From equation (1.7), it can be observed that the plasma frequency is directly proportional to the square root of carrier concentration (n) and inversely proportional to the square root of the effective mass of electron (m_e^*). Therefore, plasmon frequency can be adjusted by tailoring the charge carrier concentration and effective mass of electrons.

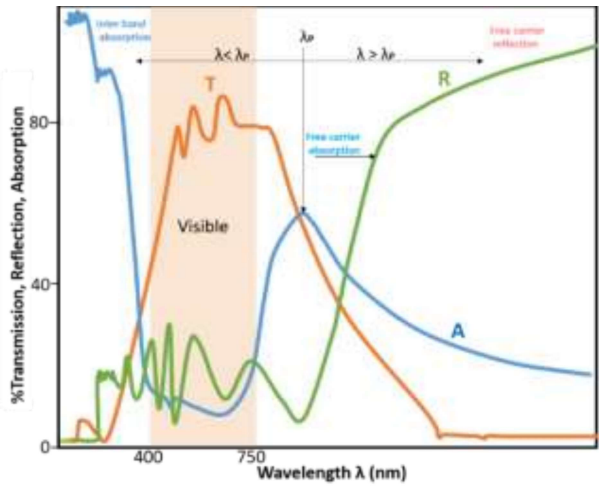

Figure 1.4 Transmission, reflection and absorption spectra of a typical TCO [2]

1.4 Effect of doping on the bandgap

Interband transitions take place in non-degenerate semiconductors from the valence band to the conduction band in direct bandgap semiconductors. In indirect bandgap

semiconductors, extra plasmon energy is required for the band-to-band transition. The n-type TCOs are generally heavily doped degenerate semiconductors, where the bottom levels of the conduction band minima (CBM) are occupied by the electrons; as a result, the Fermi level resides inside the conduction band minima. This effect is generally known as Burstein-Moss band filling. Due to the Burstein-Moss band filling, the lowest allowed transition is shifted to the higher levels of the conduction band. In such cases, the fundamental bandgap E_g is no longer the same as the optical bandgap E_g^{opt}.

1.4.1 Burstein-Moss shift

It was observed in heavily doped n-type semiconductors that the Fermi level is pushed inside the conduction band, and the vacant states of CBM are occupied. This results in the widening of the optical bandgap (E_g^{opt}), the effect is known as the Burstein-Moss shift **Figure 1.5(b)**. The Burstein-Moss shift can be given by:

$$\Delta E_{BM} = \frac{h^2}{8\pi^2}(3\pi^2 n)^{\frac{2}{3}}\left(\frac{1}{m_e^*} + \frac{1}{m_h^*}\right) \qquad 1.7$$

where $m_e^*$and m_h^* are the effective mass of electrons and holes, while h is Plank's constant, and n is the electron density.

The condition for the Fermi level to be shifted above the conduction band minimum is given by Mott-Edwards-Sienko (MES) criteria (equation 1.9):

$$a^* n_c^{1/3} \geq 0.2 \qquad 1.8$$

where a^* is the Bohr radius for an isolated donor, also known as the effective radius, for example, as in the case of Al-doped ZnO, it is presumed that the position of the Al^{+3} donor (impurity) states merge with the host (ZnO) CBM. The critical electron

concentration (n_c) obtained for Al-doped ZnO is 6.41×10^{18} cm^{-3}. If the free carrier concentration exceeds the critical Mott-Edwards-Sienko(MES) carrier concentration ($n > n_c$), the Fermi level lies above the CBM. If $n < n_c$, the Fermi level lies within the bandgap [39].

1.4.2 Bandgap narrowing

The bandgap of semiconductors can be reduced by exchange interaction between the charge carriers. There are mainly three types of exchange interactions in n-type semiconductors:

a. The exchange interaction between electrons: The electrons repel each other, which is given by e^2/r. As a result, electron of like spin tends to keep away from each other, reducing the repulsive energy, which tends to bring down the conduction band minima towards lower energies.

b. When an electron is excited to a higher energy state, it leaves behind a hole. The electrons and holes attract each other and arrange themselves in such a way as to minimize their energy. Due to this rearrangement, the valance band maximum is moved to higher energies.

c. When impurity atoms are ionized, they become positively charged and tend to gather electrons around them. This type of interaction tends to shift CBM to lower energies, as shown in **Figure 1.5(c)**

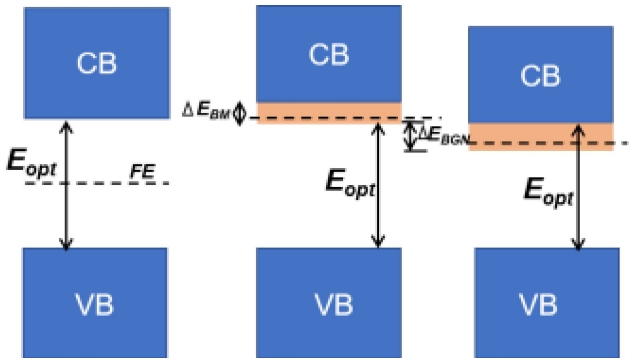

Figure 1.5 Optical Bandgap of semiconductor, a) Burstein Moss BM) shifting after dopant addition, and b) Bandgap narrowing (BGN) after dopant addition c)

Therefore, the total or effective bandgap can be given by:

$$E_{eff} = E_o + \Delta E_{BM} - \Delta E_{BGN} \qquad 1.9$$

Therefore, doping is very important for TCO as it allows bandgap tuning [40], and increases charge carrier.

1.5 ZnO-based TCO

ZnO as a thin film was first prepared in 1959 by Heiland et al.[41] by evaporation of the Zn metal followed by oxidation. Mickelsen et al. [7] reported optical transparency and conductivity in 1966 by reactive sputtering of zinc metal on a glass substrate in an oxygen-argon atmosphere. Obtained conductivity was 10^{-4} S/cm, while the absorbance was ~0.001 in the visible range. The first solution-based spray-deposited film of ZnO on a fused quartz substrate was reported [8] with a conductivity of 0.03 S/cm and transmittance of about 95%. Since then, there has been a huge interest in the optoelectronic properties of zinc oxide. The increase in the number of publications over the last two decades (**Figure 1.6**) is a testament to the interest.

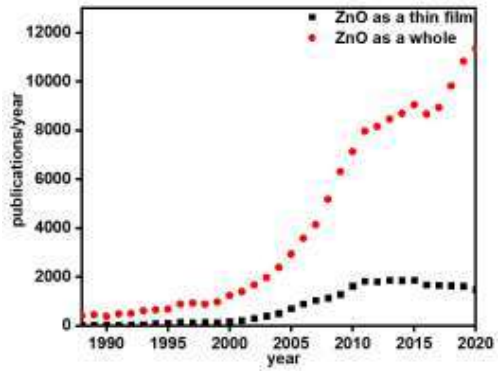

Figure 1.6 Zinc oxide articles published using ZnO as a bulk material and as a thin film. (Data taken from Scopus dated 20/02/2022 using the keywords "zinc oxide" and "zinc oxide and aluminium doped zinc oxide thin films")

1.6 Structural and chemical properties

Zinc oxide occurs naturally as mineral zincite and crystallises as a hexagonal wurtzite structure ($P6_3mc$) [42]. Bragg first determined the crystal structure of ZnO during World War I [43]. Zinc oxide can assume three different crystal structures: cubic zinc blende type structure, hexagonal wurtzite or rock-salt type structure, depending on the stacking sequence of the bi-layers, as shown in **Figure 1.7**. The bond formation energy is the lowest when ZnO assumes the wurtzite crystal structure (**Table 1.1**); therefore, in ambient conditions, wurtzite is the thermodynamically stable phase [44] as shown in **Figure 1.7a**. Due to the missing inversion symmetry, the wurtzite ZnO unit cell can be imagined as Zn atoms or oxygen atoms terminated basal plane (001). This leads to a strongly different etching behaviour of both planes, an effect used to prepare textured ZnO films for improved light scattering [45]. On the other hand, Zinc blend structure can be regarded as an arrangement of two interpenetrating face-centred cubic sub-lattices

displaced by ¼ of the body diagonal axis. The bonding orbitals are directed along the four body-diagonal axes as shown in **Figure 1.7b**.

Table 1.1 ZnO polymorph space group, lattice constant, bond energy, and formation energy

Crystal Structure	**Hexagonal**	**Zinc blende**	**Rock-salt**
Space Group	$P6_3mc(186)$	$F\bar{4}3m(216)$	$Fm\bar{3}m(225)$
Lattice Constant	a=b=0.3249nm c=0.52042 nm	a=b=0.4463 nm	a=b=c=0.4316nm
Bond Energy (eV)	-7.692 eV	-7.679 eV	-7.455 eV
Total Formation Energy (eV)	-5.658 eV	-5.606 eV	-5.416 eV

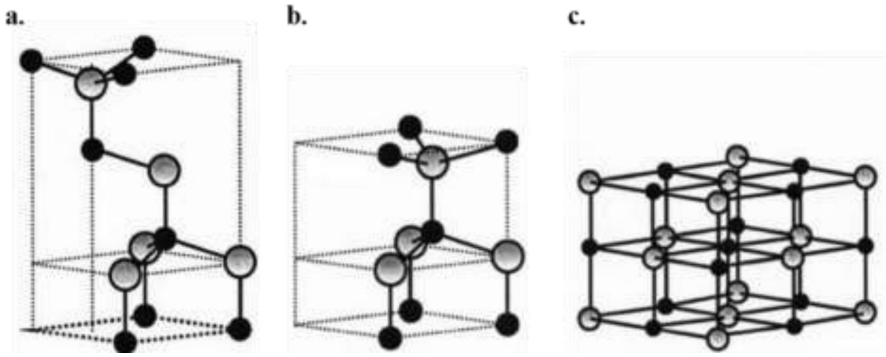

Figure 1.7 Zinc oxide polymorphs a) zinc blende, b) wurtzite, and c) rock-salt Reproduced with permission[46].Copyright 2012,Springer

Zinc blend structure is generally formed when ZnO epitaxial films over compatible substrates such as GaAs or ZnS. At higher pressure of around 10 GPa, the ZnO assumes a rock-salt crystal structure, as shown in **Figure 1.7c**. Intrinsic ZnO is generally n-type, due to the presence of defects such as zinc interstitials and oxygen

vacancies. However, by changing the type of defect and dopants, ZnO can be made n-type or p-type. In general, the resistivity of undoped ZnO thin films varies from ~10^{2} [47–51] to ~10^{-2} Ω-cm [52,53], depending upon the processing techniques, substrate, and defects.

1.7 Defects in ZnO

Defects play an important role in deciding the electrical and optical properties of TCOs. For ZnO, the prominent defects include vacancies of oxygen (V_o), zinc (V_{Zn}), zinc and oxygen interstitials Zn_i, O_i, and antisite defects (regular position interchanged by another atom) such as O_{Zn} and Zn_O [54]. Apart from these, stoichiometric Schottky (cation and anion vacancy) and Frenkel (cation vacancy and cation interstitial) defects can also be present in ZnO. These defects play an important role in modifying the electrical and optical properties. The type and concentration of defects depend on the processing history and environment, in turn affecting the photo luminescence, carrier migration, and lifetime. Local deformities have been accepted to play a more significant function in ZnO, which regularly shows elevated levels of accidental n-type conductivity. V_o and Zn_i have been frequently identified as the root cause of n-type conductivity in ZnO [22].

Oxygen vacancy (V_O) is the most viable defect in ZnO. It has been the most discussed as a major cause of n-type conductivity in intrinsic ZnO. V_O has the minimum formation energy in zinc-rich conditions compared to other imperfections in **Figure 1.8a**. Earlier, it was considered an important source of n-type conductivity. However, recently, V_O been found to be a deep donor [54]. It has been confirmed that the formation energy of V_o^{++} is close to the valence band maximum,

the neutral state (V_O) is in the mid-bandgap, while V_o^+ is more stable near the conduction band minimum. Therefore, it was concluded that the vacancy of oxygen being a deep-level donor doesn't have a major contribution to n–type conductivity of ZnO. Zinc interstitials (Zn_i) generally occupies an octahedral site in the wurtzite structure [55,56], while Zn_i at a tetrahedral site is less thermodynamically favored. The Zn_i is a shallow donor, with a donor energy of 30 meV below the CBM[57]. It has also been found that the thermodynamic transition levels show stability with the one-electron structure near the conduction band minima. The Zn_i possesses a very small relocation barrier of the order of 0.57 eV for the "2+" charge state[56]. Hence, it is required to diffuse out effectively or bind with different imperfections [54].It is much more common that acceptor-type defect creation requires lower formation energy of ~0.8 eV in n-type ZnO in oxygen-rich conditions. However, in the zinc-rich case, it has very high formation energy of ~ 4-8 eV making it rather difficult to occur, as shown in **Figure 1.8b**. The formation energy changes with the fermi energy level. As V_{Zn} gives p-type characteristic property to the ZnO lattice can easily counteract the existing n-type characteristics. Zinc vacancy leaves four unbounded oxygen. As a result, six electrons remain in the vicinity of a Zn vacancy. These four O dangling bonds consolidate into a doubly involved symmetric "a_1" state found somewhere down in the valence band and three practically degenerate states in the bandgap near the valence band maxima (VBM)[54,58].

Oxygen interstitial and antistites are the other possible point defects in zinc oxide. These defects are difficult to form due to the higher formation energy. Its formation

is not generally viable in regular processing routes but oxygen-rich conditions, as shown in **Figure 1.8(b)**.

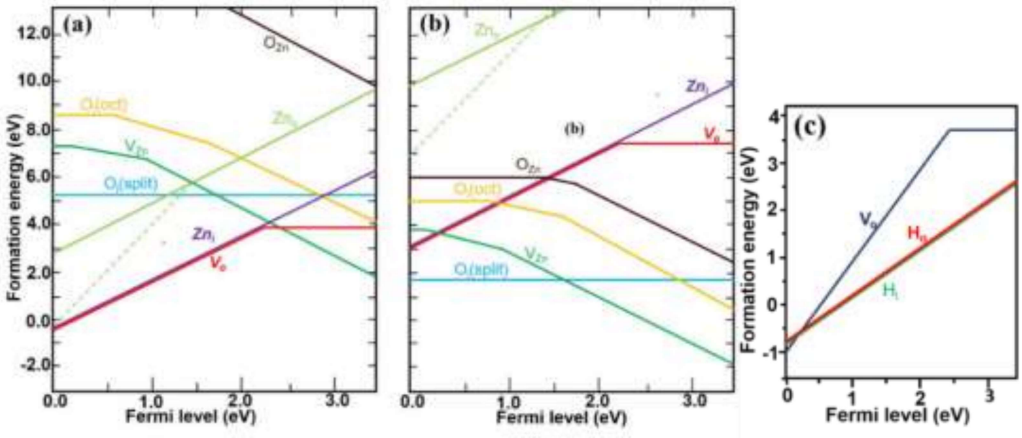

Figure 1.8 Formation energies as a function of Fermi-level position for native point defects in ZnO for (a) Zn-rich and (b) O-rich conditions (c) in presence of hydrogen[54]

When ZnO film is annealed in the presence of hydrogen, hydrogen goes into interstitials (H_i) and acts as a shallow donor, as shown in **Figure 1.8(c)**. The zero of the Fermi level corresponds to the conduction band minima. Only segments corresponding to the lowest energy charge states are shown in **Figure 1.8**. The slope of these segments indicates the charge state. Kinks in the curves indicate transitions between different charge states.

The unintentional intrinsic defect density is generally lower; therefore, these intrinsic defects play a minor role in inducing n-type conductivity in real applications. Therefore, some impurity atoms, having different valencies, are intentionally added to induce n or p-type characteristic properties. These impurities act as shallow donors or acceptors and play a major role in electrical conductivity. For inducing, the n-type character in ZnO, Group -IIIA elements B, Al, Ga, or In

are substituted on the Zn sites [59]. When a group IIIA element is substituted for Zn in the lattice, the extra valance electron remains unbounded and has energy very close to the conduction band minima. When enough concentration of a group IIIA element is added (usually 1-3 at%) filling the lower levels of CBM, as a result, the Fermi level shifts into the CB (also known as BM shifting). In such cases, enough population of electrons in the CB is there and doped ZnO behaves like a conductor.

1.8 n-type dopants

The most popular dopants for n-type ZnO have been the group IIIA elements such as Ga, In, Al, and B. Doping with these elements increase the carrier concentration by donating one electron close to the conduction band; thereby increasing the optical bandgap and transparency range. Al is the cheapest and most earth-abundant option.

Aluminum

Aluminum is an IIIA group element. The low ionization energy of Al (~120 meV) and a low formation energy requirement for Al substitution for Zn in the ZnO lattice make it the most favorable n-type dopant for ZnO. Aluminum substituted for Zn in the ZnO lattice acts as a shallow donor and gives a free electron [60]. On doping Al, the bandgap of ZnO increases [61–63] due to Burstein-Moss Shifting. Preferential orientation along [002] direction has been observed to improve on doping Al, while at the same time, Al also tends to segregate towards the grain boundaries, especially in solution-processed films [64]. Contradictory effects of Al doping on grain size have been observed. While the grain size of zinc oxide films

was found to increase on aluminum doping [65,66] up to a certain concentration, in some cases, the grain growth was inhibited due to the formation of alumina at grain boundaries [32,67–69]. Doping improves electrical conductivity; however, excess doping beyond a level results in charge carrier scattering and a reduction in mobility, thereby deteriorating electrical conductivity [70].

Indium

Indium is another popular dopant for ZnO. Indium is also a IIIA group element, which donates a free electron. Having an ionic radius (0.80 Å) comparable to Zn^{+2} (0.74 Å), In^{+3} doping does not result in strain in the lattice; thereby, greater mobilities are achieved. Resistivity values lesser than 10^{-4} Ω-cm and transparency ~90% have been demonstrated in thin film indium doped ZnO [71]. Indium is found to favor the (101) orientation in ZnO thin films [72].

Gallium

Gallium is another group IIIA element and a popular dopant for ZnO, which has an ionic radius close to 0.62 Å. The major benefit of Ga over Al is the lower affinity for oxygen. The chance of formation of Ga_2O_3 is lesser than Al_2O_3, as the formation energy of Ga_2O_3 (−11.29 eV) is much less negative when compared to alumina (-17.27 eV), which makes it a more stable dopant. Resistivities of the order of ~10^{-4} Ω-cm has been reported for Ga-doped ZnO films processed through aerosol-assisted chemical Vapor deposition (AACVD) [73,74], sputtering [75] and atomic layer deposition (ALD) [76]. In comparison, resistivity values in the order of ~10^{-3} Ω-cm have been reported using solution-based approaches [77].

Hydrogen

Hydrogen is thermodynamically stable in ZnO lattice at interstitial sites in the form of H_i^+. Therefore, n-type conductivity can be improved by doping hydrogen in ZnO. Hydrogen readily substitutes oxygen vacancy and acts as a shallow donor [78]. It has been demonstrated that hydrogen tends to passivate defects such as oxygen and zinc vacancies and Zn interstitial. In addition, hydrogen acts as a shallow donor, thereby improving the conductivity. By hydrogen incorporation, resistivities as low as $\sim 10^{-4}$ Ω-cm has been achieved in the AZO films [79]. Although hydrogen incorporation has been studied in sputtered films [15,79], reports on hydrogen treatment of solution-processed films are scarce.

Fluorine

Fluorine (F) doping in ZnO substitutes oxygen in the lattice to give a free electron. It was observed that up to a certain concentration, F doping results in bandgap widening. However, beyond the limit, F does not show much effect on the bandgap, at the same time, orientation was observed to deteriorate, while mobility was reduced [80–82].

Thallium

Thallium (Tl) has recently been projected as a viable co-dopant for Al-doped ZnO[83,84]. Similar to aluminum, Tl substitutes zinc in the ZnO lattice. Its iso-valent nature forms an electron cluster through which faster transfer of electrons takes place. The difference in electronegativity of Tl and Al helps in improving the

carrier concentration[85]. Tl being less electronegative than oxygen helps in electron density increases near oxygen. In addition, the thallium cooping helps in improving the mobility of AZO films [84,86].

1.9 Motivation

By the year 2027, the TCO market is expected to be worth ~$10 billion. The current market share of ITO in the TCO business is >80% [87,88]. As indium resources are limited, the search for TCO systems comprising earth-abundant elements is gaining pace. Zinc and aluminum being earth-abundant elements, ZnO-based, more particularly AZO (aluminum-doped zinc oxide), is being explored as an alternative to the ITO.

ZnO-based TCO has been shown to have properties comparable to that of ITO [89,90]. However, these high-transparency and low-resistivity ZnO-based TCOs were processed through vapor-based processing routes, most prominently, sputtering and PLD. However, these vapor-based processing methods involve high installation and maintenance costs, and cannot be easily adapted to large-scale industrial production. Therefore, high-throughput and cheaper processing techniques are being sought.

Solution-based processing, such as spray pyrolysis or sol-gel-based coating technologies, is much cheaper and can easily be adopted in roll-to-roll/large-scale industrial production lines. However, the ZnO-based TCOs processed through these solution-based processing routes exhibit much inferior electrical and optical properties when compared with that processed through sputtering or PLD.

Therefore, in order to adopt these solution processing routes for processing ZnO-based TCO, achieving properties comparable to the Vapor-based routes is vital. The first step would be to understand the major reasons for the lower performance of the solution-processed films and mitigate these factors. This, followed by devising strategies to improve the electrical and optical properties in solution-processed films, would pave the way towards adopting solution-based processing for large-scale production of ZnO-based TCOs.

It has been established that the solution-processed Al-doped ZnO films generally end up with impurities/undecomposed precursors, smaller grains, inactive dopants, and random orientation. Therefore, post-deposition annealing is generally required [2,91,92].Several annealing strategies have been devised including vacuum annealing[22,33,93], annealing in reducing [39,91,94–96] and inert atmosphere[66] and radiative annealing[97,98]. The role of defects, their interaction with dopants in the lattice, and the orientation of the deposited films are other important factors that decide the properties of AZO films. Many in-depth studies on the role of defects, their interaction, and their orientation have been published. However, not many in-depth studies have been published on the role of defects, their interaction, and strategies to improve carrier density, mobility, dopant activation, and defect passivation to improve the performance of solution-processed ZnO-based TCOs.

1.10 Organization of Thesis

The first chapter is introductory, giving an overview of the fundamentals of transparent conductive oxide, structure, and relevant properties of ZnO, intrinsic and extrinsic defects i.e. produced by doping in ZnO-based TCOs and undergoing

processing routes. The chapter also briefly explains the importance and motivation behind undertaking this thesis work.

In the second chapter, a discussion on the existing processing routes for Al-doped ZnO-based TCOs is presented. Both vapor-based and solution-based processing technique and their major advantages and disadvantages are briefly discussed. State-of-the-art in each processing route is also outlined. Different post-deposition annealing technique and their effect on the electrical and optical properties of AZO TCOs are also discussed.

The third chapter deals with the experimental and characterization techniques utilized during this thesis work. The processing method and important processing parameters and protocols are described, along with the main characterization techniques adopted for evaluating the structure and performance of the deposited Al-doped ZnO TCO.

The fourth chapter discusses the microstructure and defects formed during the AZO film fabrication via spin coating. The role of orientation, defects, and grain boundaries in deciding the electrical and optical properties of the AZO thin film is discussed.

In the fifth chapter, spray pyrolysis deposition of AZO film is described. The improvement in film microstructure and enhancement in defect and carrier density through vacuum annealing. The role of vacuum annealing in terms of mobility, electrical conductivity, and optical transparency has been characterized and discussed in depth.

The sixth chapter discusses the effect of radiative annealing on the optoelectronic properties of solution-spray-deposited Al-doped ZnO. This chapter discusses the effect of hydrogen as a shallow donor and its passivating effect on the vacancy of oxygen and zinc interstitial, at the same time improving the transparency and conductivity.

The seventh chapter discusses the effect of co-doping Tl in AZO and radiative annealing in hydrogen. The effect of the presence of a large Tl atom on the mobility is evaluated, and the role of thallium in improving the electrical conductivity and transparency of the film is discussed.

The eighth chapter discusses the overall summary and conclusions. Prospects of solution-processed Al-doped ZnO are also discussed.